Proceedings of the ASME 2012 10th International Conference on Nanochannels, Microchannels, and Minichannels
ICNMM2012
July 8-12, 2012, Rio Grande, Puerto Rico

ICNMM2012-73142

An Electrowetting-Based Technique for Hot-Spot Cooling of Integrated Circuits: Experimental and Numerical Approach

S. Alavi
Graduate Student
sina.alavi@stu-mail.um.ac.ir

S. A. Kazemi
Graduate Student
ali.kazemi@stu-mail.um.ac.ir

M. Passandideh-Fard
Associate Professor
mpfard@um.ac.ir

Micro/Nanofluidics Laboratory (MNL), Ferdowsi University of Mashhad, Mashhad, IRAN

ABSTRACT

In this paper, a new method of cooling hot-spots in electronic devices is proposed based on the electrowetting phenomenon. Since the microprocessor technology is developing with a fast rate, conventional cooling methods for integrated circuits will eventually fail to address the needs for high performance computers. As a result, novel methods of cooling must be developed. In this study, a layer with variable and programmable thermal conductivity is placed between the electronic device and a conventional cooling system. This layer is composed of an array of liquid metal drops which can be actuated with the electrowetting phenomenon. The conductivity of this layer can be modified according to the heat transfer requirements of the system in the desired region. This action is accomplished by actuating the drop in that region with an applied AC voltage. To test the possibility of designing such a system, experimental and numerical investigations with different scenarios have been presented and compared in this paper. Two mercury drops with different volumes of 2.8 μL and 6 μL are used in a PCB-based experimental setup to observe the changes in contact angle and apex of the drops under an applied voltage. Also, the Navier-Stokes equations along with the energy equation are solved to investigate the effectiveness of the drops in cooling the hot-spots.

KEYWORDS: Hot-Spot Cooling, Electrowetting, Thermal Management, Integrated Circuits, Contact Angle, VOF method.

1. INTRODUCTION

In recent years, thermal management has become an important parameter in designing and manufacturing high-performance electronic devices including microprocessors. Based on the researches published as the International Technology Roadmap for Semiconductors (ITRS) [1], the size of the transistors in microprocessors will continually decrease over time and reach to a value of 10 nm until 2018. However, the size of the chips will remain constant and, therefore, the concentration of transistors will increase. Moreover, the ITRS has shown that the power consumption of the high-performance personal computers will experience a 92% increase until 2016. Although these changes will lead to more complicated microprocessors with improved calculation abilities, the generated heat will be dissipated from a much smaller surface area. As a result, old fashioned cooling methods such as heat sink-fan will be eventually inefficient, since they can only dissipate a constant amount of heat flux from the entire surface area of the electronic chips. This method of cooling leads to the formation of large thermal gradients, mostly known as hot-spots, which are not desired due to the associated high thermal stresses.

Some investigations have been carried out recently to design novel methods of cooling. Some of these methods include heat pipes, thermo-siphons, thermoelectric systems, etc. Also, some MEMS-based methods such as microchannels, microjet cooling [2] and microfin array heat sinks [3] have been developed. An alternative to these cooling methods are the drop-based microfluidic devices where discrete drops are actuated over an array of electrodes based on the electrowetting phenomenon.

Electrowetting is a phenomenon in which the contact angle of a polarizable or conductive liquid drop is changed by employing an electric field that leads to the movement of the drop. This technique has significant applications in the area of digital microfluidics and lab-on-a-chip devices. The phenomenon of electrocapillarity was first introduced by Gabriel Lippmann [4]. Pollack et al. [5] later demonstrated that electrowetting can serve as a useful technique to manipulate drops. Moreover, some novel studies have been carried out over the past decade to investigate the fundamental issues regarding this phenomenon such as hydrophobic coatings, contact angle variations and various electrode shapes [6-10]. Using the Volume-of-Fluid (VOF) technique in a numerical approach, Alavi et al. [11] solved for the Navier-Stokes equations along with the electrostatic equations to model the contact angle changes of sessile drops under the effect of applied voltages and compared the results with those of the experiments. More information regarding the electrowetting phenomena and the recent development in that field can be found elsewhere [12, 13].

While the most extensive application of electrowetting is in the field of biology and chemistry as in the lab-on-a-chip technology, this phenomenon has found its way in the field of chip cooling and thermal management of electronic devices [14]. Based on this technique, efficient and high performance thermal management systems allow the electronic devices to work with a higher performance.

Recently, a number of novel techniques for thermal management of Integrated Circuits (ICs) have been proposed based on the technology of Electrowetting on Dielectric (EWOD). Paik et al. [15] for the first time demonstrated the ability of micro-sized drops to cool a hot-spot using a novel coplanar electrowetting setup, which eliminated the need for a confining top plate. In addition, Mohseni [16] proposed cooling with liquid metal drops instead of water and showed that the heat transfer can be enhanced by two orders of magnitude.

A state-of-the-art system was designed by Paik [17] to employ the electrowetting phenomenon using Printed Circuit Boards (PCBs) to cool the hot-spots in integrated circuits. He showed that a hot-spot located in an array of electrodes, with a heat flux of 30 W/cm^2 can be efficiently suppressed by transporting a 6 μL water drop across the array. Later, Cheng and Chen [18] used a similar approach to cool hot-spots adaptively. Oprins et al. [19] using the FLUENT software showed that circulations inside the drops are the cause of heat transfer enhancement in these kinds of hot-spot cooling systems. They modeled the drops between two parallel plates but did not solve for the electric potential.

In this study, we propose a new method for the treatment of hot-spots in electronic devices. In this method, a layer including a liquid metal drop (such as mercury) is designed to be placed between the cooling target and a conventional cooling system such as a heat sink-fan (HSF). By actuating the drop using an electrowetting mechanism, the rate of cooling can be increased. Detailed descriptions of the system in addition to the experimental and numerical results are discussed in this paper.

2. HOT-SPOT COOLING TECHNIQUE

As mentioned earlier, due to the non-uniform heat dissipation from the transistors, hot-spots may appear on the surface of the electronic devices. This phenomenon only happens when an old-fashioned cooling system is used which can dissipate a constant value of heat flux from the entire surface of the device. This fact is explained by Paik et al. [20]. However, if a mechanism is designed such that the conductivity between the cooling target and the cooling system is changed according to the dissipated heat, then the temperature distribution would be uniform and the hot-spot would disappear. Based on the EWOD technique, Paik et al. [20] proposed a method to design such a system. For this purpose, consider the schematics shown in Fig. 1. A liquid metal drop is placed between two plates to form an interface between the cooling target and the conventional cooling system. By default, a voltage is applied between the drop and the electrode which is located at the bottom of the drop. As a result of electrowetting phenomenon, the contact angle of the drop is reduced because of the applied voltage and the drop is detached from the top plate. In this condition, the heat is conducted between the electronic device and the cooling system with the equivalent conductivity of the liquid metal and the surrounding air. This value of thermal conductivity is less than that of the liquid metal itself. Now, if more heat conduction is needed, the voltage can be removed to let the drop attach to the top plate. This act results in a significant increase of the thermal conductivity.

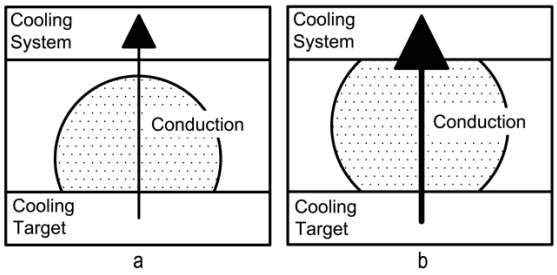

FIGURE 1. Schematics of the EWOD-based cooling method using liquid metal drops. At first, the drop is detached from the top plate (case a). If more heat conduction is needed, the voltage can be removed to let the drop attach to the top plate (case b).

An array of these cells can be arranged to form a layer with a programmable conductivity which can be modified according to the amount of desired heat transfer between the heat-dissipating target and the cooling device. Therefore, when a hot-spot forms on the surface of the electronic device, the conductivity can be increased by letting the drop attach to the top plate to suppress the hot-spot in that region. The main advantage of this system is that it can work in a combination with an old-fashioned cooling system with no need for a complete change of the system design.

In the following sections, the experimental and numerical methods are presented to test the possibility of designing the introduced technique for cooling hot-spots.

3. EXPERIMENTAL METHOD

A PCB-based experimental setup is designed to actuate the drops using the electrowetting phenomenon. The schematics of the setup can be seen in Fig. 2.

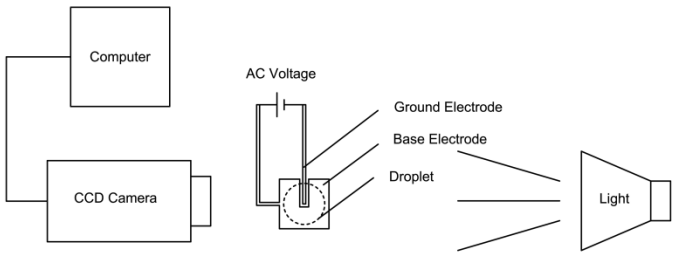

FIGURE 2. Schematics of the experimental setup for collecting the values of the contact angle, the contact radius and the apex of drops.

Since the drop must be in permanent contact with the ground electrode, this electrode is placed under the drop in the same plane with the actuating electrode. This design facilitates the actuation process and the ground electrode will not interfere with the movement of the drop. Also, a solder-mask layer of thickness 20 µm is coated and baked on the top of the actuating electrode to serve as the dielectric. A high-speed CCD camera (Grasshopper, Point Grey Inc.) mounted with a telecentric microscope lens (EC-M55, Computar Company) is connected to a computer to capture and collect the images. In addition, a diffuse light is placed on the opposite side with regard to the camera such that the interface of the drop will be sharp enough for further image processing. The captured images are subsequently used to obtain the required data. This procedure is shown in Fig. 3. To calibrate the measurements, a precise needle with the diameter of 0.6 mm is placed near the drop and all the measurements are carried out in comparison with the needle. Using the AutoCAD software, a spline is fitted to the free surface to obtain the profile and volume of the drop. Similarly, the values for the contact angle, the contact radius and the drop apex can be obtained from the images. Depending on the resolution of the images, the accuracy of the measured dimensions is about 20 µm to 30µm.

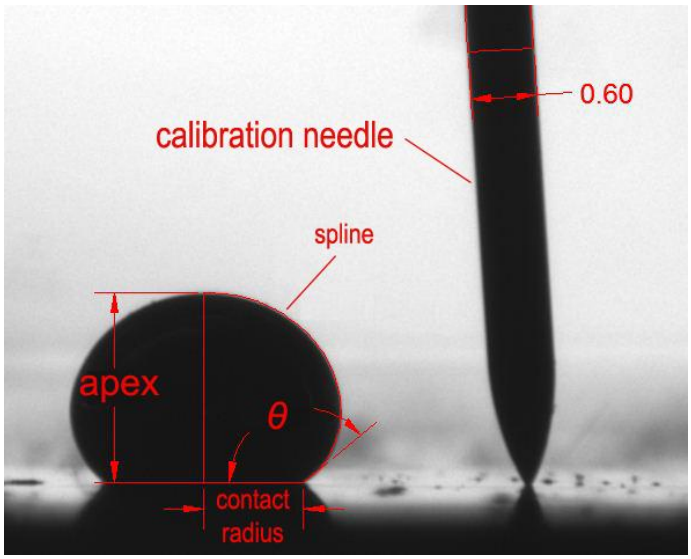

FIGURE 3. The method of obtaining data from the images and calibration process.

During the experiments, for each size of the drop, first a voltage of 240V is applied to the electrode to change the contact angle and an image is taken from the drop. Next, the voltage is removed and another image is captured. This process is repeated five times to observe the repeatability of the method for later use in the hot-spot cooling process and to study the effects of contact angle hysteresis.

4. NUMERICAL METHOD

4.1. Fluid flow

The Navier-Stokes equations are solved in a 2D axisymmetric domain to model the electrowetting phenomenon. Considering

the flow to be incompressible, laminar and Newtonian, the continuity and N-S equations will become:

$$\nabla \cdot \vec{u} = 0 \tag{1}$$

$$\frac{\partial \vec{u}}{\partial t} + \nabla \cdot (\vec{u}\vec{u}) = -\frac{1}{\rho}\nabla P + \frac{1}{\rho}\nabla \cdot \vec{\tau} + \frac{1}{\rho}\vec{F}_b \tag{2}$$

in which $\vec{u}$ is the velocity vector, $\rho$the density, $\mu$the dynamic viscosity, $P$the pressure and $\vec{\tau}$ is the stress tensor defined as:

$$\vec{\tau} = \mu[(\nabla \vec{u}) + (\nabla \vec{u})^T] \tag{3}$$

The body forces $\vec{F}_b$ include the gravity and surface tension forces. A three-step projection method [21] is employed to solve the continuity and momentum equations simultaneously in three fractional steps. In this manner, the first step includes obtaining an interim velocity $\vec{u}^{\,n+\frac{1}{3}}$ by discretizing the convective and body force terms explicitly, as follows:

$$\frac{\vec{u}^{\,n+\frac{1}{3}} - \vec{u}^{\,n}}{\delta t} = -(\vec{u} \cdot \nabla \vec{u})^n + \frac{1}{\rho^n}\vec{F}_b^n \tag{4}$$

Moreover, the viscous terms are discretized implicitly. This treatment leads to obtaining a second interim velocity in the next step as:

$$\frac{\vec{u}^{\,n+\frac{2}{3}} - \vec{u}^{\,n+\frac{1}{3}}}{\delta t} = \frac{1}{\rho^n}\nabla \cdot \left[\mu\left[\left(\nabla \vec{u}^{\,n+\frac{2}{3}}\right) + \left(\nabla \vec{u}^{\,n+\frac{2}{3}}\right)^T\right]\right] \tag{5}$$

Since the interim velocity $\vec{u}^{\,n+\frac{2}{3}}$ exists at both sides of the relation, the method of TDMA (Tri-Diagonal Matrix Algorithm) is used to obtain the interim velocity at this step.

Finally, in the third step, the interim velocity $\vec{u}^{\,n+\frac{2}{3}}$is projected to a divergence-free velocity field, defined as follows:

$$\frac{\vec{u}^{\,n+1} - \vec{u}^{\,n+\frac{2}{3}}}{\delta t} = -\frac{1}{\rho^n}\nabla \cdot P^{n+1} \tag{6}$$

In combination with the continuity equation, this relation yields the Pressure Poisson Equation (PPE) for the evaluation of pressure at the new time level $(n+1)$, using $\vec{u}^{\,n+\frac{2}{3}}$:

$$\nabla \cdot \left[\frac{1}{\rho^n}\nabla P^{n+1}\right] = \frac{\nabla \cdot \vec{u}^{\,n+\frac{2}{3}}}{\delta t} \tag{7}$$

The resulting set of equations is symmetric and positive definite and; therefore, the Incomplete Cholesky-Conjugate Gradient (ICCG) solver is utilized to obtain the pressure [22]. The obtained pressure is next used to calculate the final velocity at time level $(n+1)$ using Eq. 6.

4.2 Free surface tracking

The interface of the drop and surrounding gas is advected using the Volume-of-Fluid (VOF) method in a fixed Eulerian mesh. This method utilizes a scalar function f as follows:

$$f = \begin{cases} 1 & \text{inside the liquid} \\ > 0, < 1 & \text{at the free surface} \\ 0 & \text{inside the gas} \end{cases} \tag{8}$$

This function shows the fraction of a cell which is filled with liquid. Consequently, when the cell is fully occupied with liquid, the value of f will be set to unity. In contrast, an empty cell will take the value of zero, and the cells residing on the interface a value between zero and one. The values for f function are advected due the following relation:

$$\frac{\partial f}{\partial t} + \left(\vec{V} \cdot \nabla\right) f = 0 \tag{9}$$

In this equation, the Youngs PLIC algorithm is used to track the free surface of the drop [23]. Surface tension is modeled using the Continuum Surface Force (CSF) proposed by Brackbill et al. [24]. Based on this method, Aleinov and Pucket [25] suggested the following relation for the surface forces:

$$\vec{F}^{ST} = \sigma\kappa\frac{A}{V}\hat{n} \tag{10}$$

in which A is the surface area of the portion of the cell filled with liquid and V is the cell volume. $\sigma$is the surface tension and$\hat{n}$ is the unit normal directing outward the liquid, which is also used to obtain the local total curvature of the free surface as:

$$\hat{n} = \frac{\nabla f}{|\nabla f|} \tag{11}$$

$$\kappa = -\nabla \cdot \hat{n} \tag{12}$$

both defined in terms of the liquid fraction f. In addition, to apply the contact angle between the drop and the walls, the unit normal $\hat{n}$ at the vicinity of the free surface of the drop and the desired wall is changed according to the value of the contact angle.

4.3. Heat Transfer

To model heat transfer for the hot-spot cooling process, the enthalpy method is used. In this method, instead of solving the

energy equation in terms of temperature, it is formulated in terms of enthalpy. Assuming constant densities and neglecting the viscous dissipation term, the energy equation may be written as [26, 27]:

$$\frac{\partial h}{\partial t} + (\vec{u} \cdot \nabla)h = \frac{1}{\rho}\nabla \cdot (k\nabla T) \quad (13)$$

Equation 13 is only used inside the liquid, i.e. when f equals one. Otherwise, there will be an incorrect diffusion of enthalpy in the computational domain between two points with the same temperature. In other regions with a volume fraction smaller than one, energy equation in terms of temperature is used.

5. RESULTS AND DISCUSSION

5.1. Experimental Results

In this section, the results of the experiments for two drop sizes are presented. A mercury drop of volume 6 µL is placed manually on the electrode and actuated with a voltage of 240V. Mercury is chosen as the material for the drop because of its excellent characteristics both as a heat conductor and as a liquid with hydrophobic features. This selection eliminates the need for a hydrophobic coating on top of the dielectric. As a result of the voltage, the contact angle of the drop is reduced. Figure 4 shows the results of this experiment.

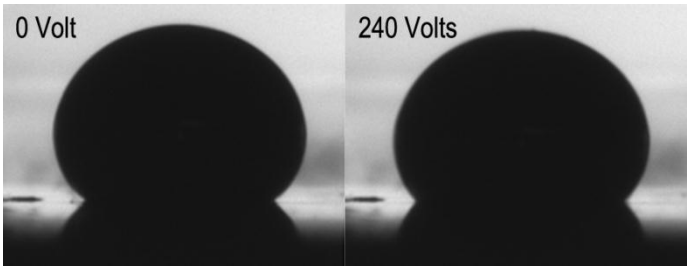

FIGURE 4. Results of the experiment for the 6 µL drop with and without an AC voltage of 240V.

The change of contact angle can be seen in Fig 5. Initially, the contact angle of the drop is measured to be 141°. As the voltage is applied, the contact angle changes to 133° and when it is removed, the contact angle changes back to 139°. However, as the experiment is repeated, the average value of contact angle at 0V approaches 141.5° and an average value of 133.8° is obtained under 240V. The difference between the measured contact angles in each case is most likely due to the contact angle hysteresis and measurement errors.

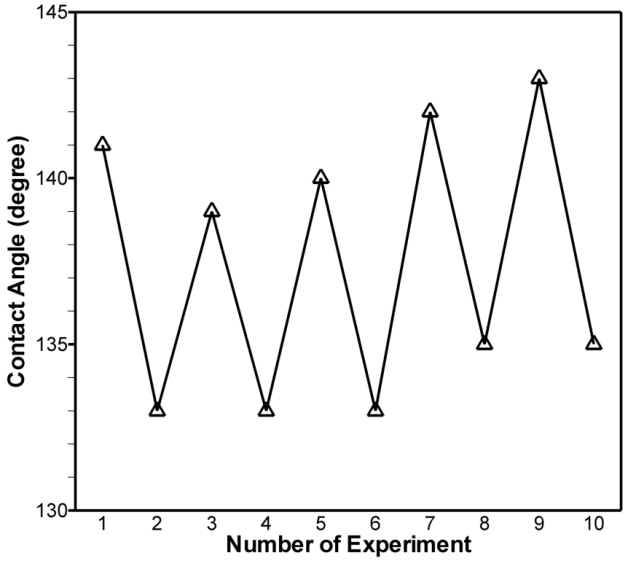

FIGURE 5. Variation of contact angle with and without the applied voltage for the 6 µL drop. The experiment is repeated 10 times to study the repeatability of the method for hot-spot cooling process.

The variation of the contact radius and the apex of the drop are depicted in Fig. 6. It is observed that when the voltage is applied, the drop further wets the surface and the contact radius is increased, while in contrast, the apex of the drop is decreased. As the experiment is repeated, it is seen that the values of contact radius and the apex of the drop nearly change between two specific values. This behavior of the drop in electrowetting phenomenon is ideal for the hot-spot cooling process.

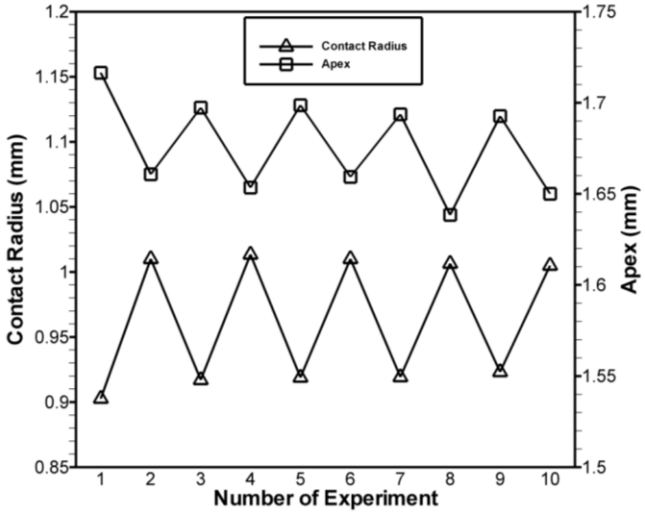

FIGURE 6. Variation of contact radius and apex of the 6 µL drop with and without the applied voltage. The experiment is repeated 10 times to study the repeatability of the method for hot-spot cooling process.

Next, the experiment is repeated for a mercury drop of volume 2.8 µL. Figure 7 shows the change of contact angle as the voltage is applied between the drop and the electrode. For the

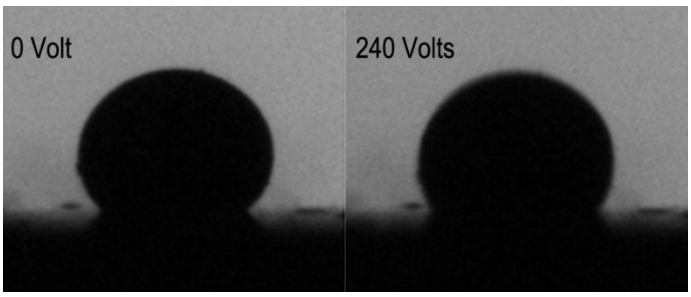

FIGURE 7. Results of the experiment for the 2.8 µL drop with and without an AC voltage of 240V.

same case, Fig. 8 shows the change of contact angle as the voltage is applied and removed. For this size of drop, the measured values of contact angle show much more inconsistency. The reason is thought to be due to the contact angle hysteresis and pinning (related to surface roughness) which both have more effects on the movement of smaller drops. More information about these phenomena is found elsewhere [28-30]. Nevertheless, when the voltage is applied for the first time, the decrease of the contact angle is measured to be from 136° to 120°, which is higher in comparison with the 6 µL drop. As seen in Fig. 8, different values of the contact angle are obtained from the measurements; this means that the experiments for this size of the drop is less repeatable compared to the previous case with a larger drop size. As a result of this behavior, using small sizes for the drop in the cooling system is not advised.

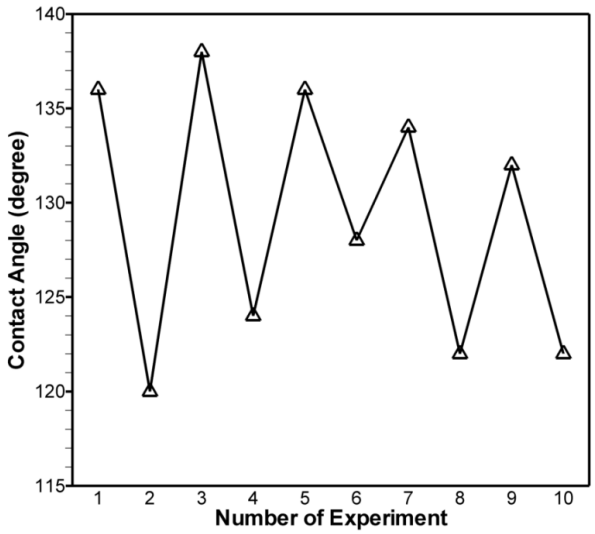

FIGURE 8. Variation of contact angle with and without the applied voltage for the 2.8 µL drop. The experiment is repeated 10 times to study the repeatability of the method for hot-spot cooling process.

The change of the contact radius and the apex of the 2.8 µL drop are shown in Fig. 9. Compared to the previous case (Fig. 6), the change of the contact radius and the apex is seen to be less repeatable; this is another indication that smaller drop sizes are not desirable for the hot-spot cooling purposes.

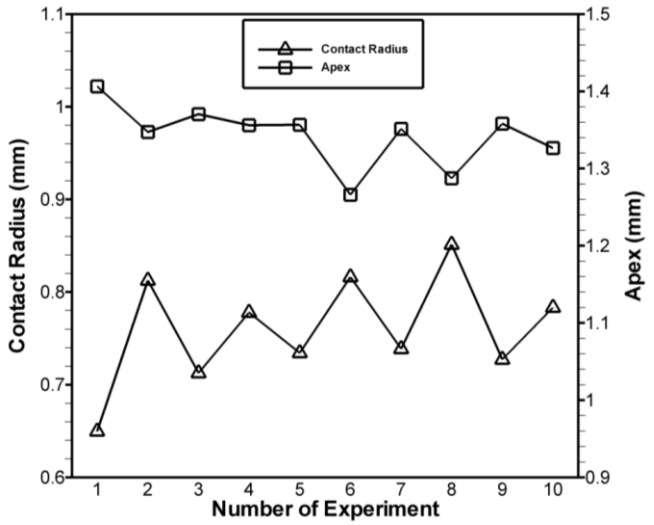

FIGURE 9. Variation of contact radius and apex of the 2.8 µL drop with and without the applied voltage. The experiment is repeated 10 times to study the repeatability of the method for hot-spot cooling process.

Based on the observations, a conclusion can be made that as the drop size decreases, the change of the contact angle and the apex under the same applied voltage increases. For the hot-spot cooling purposes, a larger change of the drop apex under a specific applied voltage is preferred. However, as discussed above, when the drop size is decreased the effects of the contact angle hysteresis and pinning will be more pronounced. As a result, the volume 6 µL for the drop is preferred to a smaller value in this study.

5.2. Numerical Results

Model Validation. In this section, simulation results are presented and compared with those of the experiments. The results of the simulations for the 6 µL drop are presented in Fig. 10. The value of the contact angle for the simulations is adapted from the experimental images. This figure shows the results for the profile of the drop before the voltage is applied with a contact angle of 141°. It can be seen that the numerical results are in a good agreement with the experimental observations. The value of the apex is predicted correctly as well.

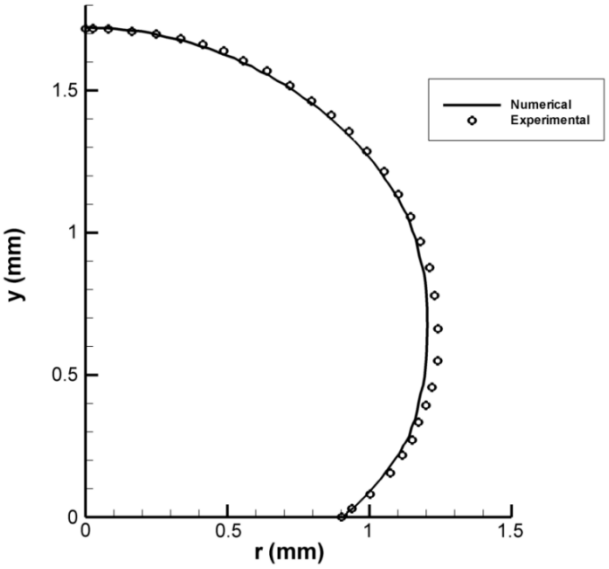

FIGURE 10. Comparison between the numerical and experimental results for the profile of the 6 μL drop before the applied voltage.

Figure 11 shows the results of the simulations for the drop in comparison with the experiments when the voltage is applied and the contact angle is decreased to 133°. The results show a good agreement for this case as well. It can be seen that as the voltage is applied to the drop, the apex of the drop is reduced.

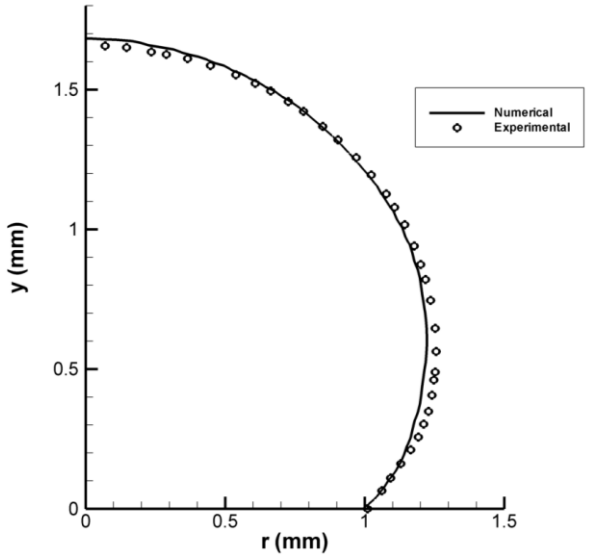

FIGURE 11. Comparison between the numerical and experimental results for the profile of the 6 μL drop after the applied voltage.

Hot Spot Cooling Scenario. Consider two parallel plates which are placed 1.8 mm apart. A drop of volume 6 μL is placed between the plates. In the absence of a voltage, the contact angle of the drop is 141° as measured in the experiments. As a result of this contact angle, the drop apex is large enough for the liquid to be attached to both plates. However, when a voltage of 240V is applied to the bottom plate, the contact angle will decrease along with the apex of the drop and, therefore, the drop will detach from the top plate. The schematics of this arrangement can be seen in Fig. 12.

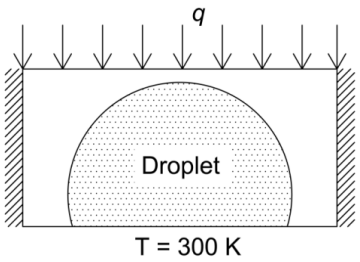

FIGURE 12. The arrangement of the hot-spot cooling process. The surface area of the top plate is $10mm^2$

A constant heat power of 1 W enters from the top plate and the bottom plate is kept at 300 K by the means of a conventional cooling system such as a heat sink-fan. Also, the side walls of the system are insulated. Because of the input heat, the temperature of the top plate will have a value of 325 K in the steady state condition; i.e. when the drop is detached and placed at rest. The temperature distribution of the top plate under this flux is shown in Fig. 13.

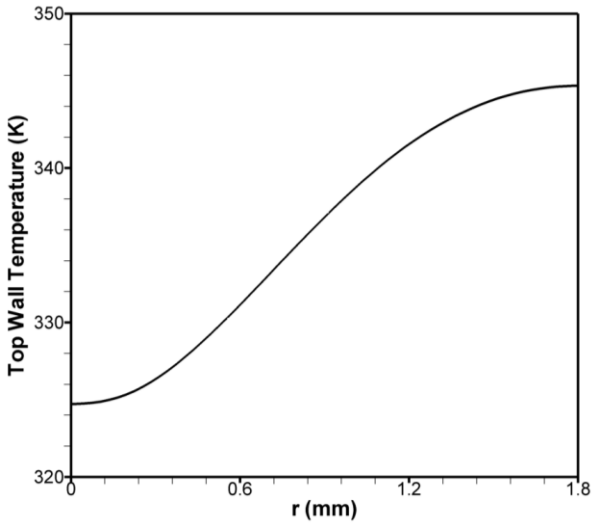

FIGURE 13. Temperature distribution of the top plate in the radial direction before the attachment of the drop, for a power input of 1 W.

Although the drop is not attached, it has affected the temperature of the top plate. As a result, the temperature of the peripheral regions of the top plate is higher than the central regions. If more heat conduction is needed to suppress a hot-spot, the applied voltage must be now removed. As a result, the drop will rise until it attaches the top plate; this will increase the value of thermal conductivity between the top and bottom plates. Consequently, this procedure leads to a better cooling of the hot-spot seen in Fig. 14.

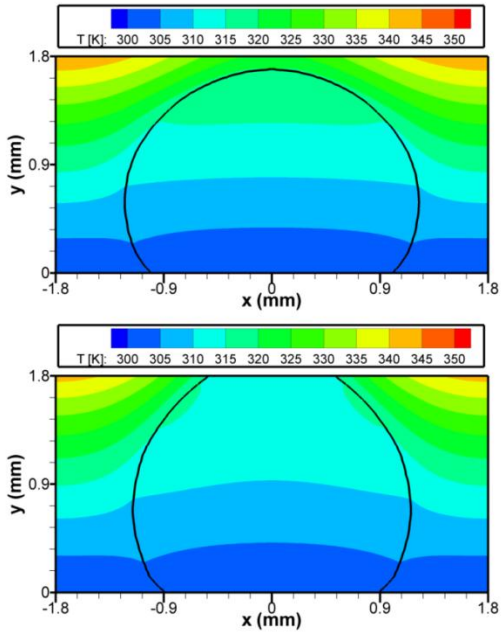

FIGURE 14. Temperature distribution of the system before (top) and after the attachment of the drop (bottom) when the voltage is removed, for a power input of 1 W. The free surface of the drop is shown with a black line inside the domain.

Figure 15 shows the variation of the steady state temperature distribution of the top plate before and after the removal of the voltage. When the voltage is applied and the drop is detached from the top plate, the temperature on the axis of symmetry ($r = 0$) is 325 K. After the drop attachment, the temperature at this point decreases to 314 K. Also in the periphery of the top plate, the temperature decrease is obtained to be about 3 K which is less than the value of 11 K on the axis of symmetry. In addition, it is observed that this temperature decrease has occurred in about 4 seconds which is a considerable short time.

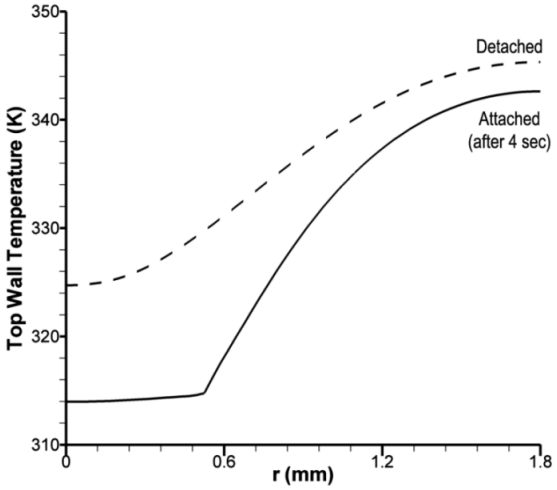

FIGURE 15. Comparison between the temperature distribution of the top plate in the radial direction before and after the voltage removal, for a power input of 1 W.

To study the effects of the heat power intensity, the power is doubled to a value of 2 W. Figure 16 shows the temperature distribution for the top wall in the radial direction during the time that the voltage is applied and the drop is not attached to the top plate. It is clear that the temperature values on the axis of symmetry and in the peripheral regions of the top wall are higher in comparison with the previous case with a power input of 1 W. An increase of 25 K can be seen on the axis of symmetry because of the increase of the power input.

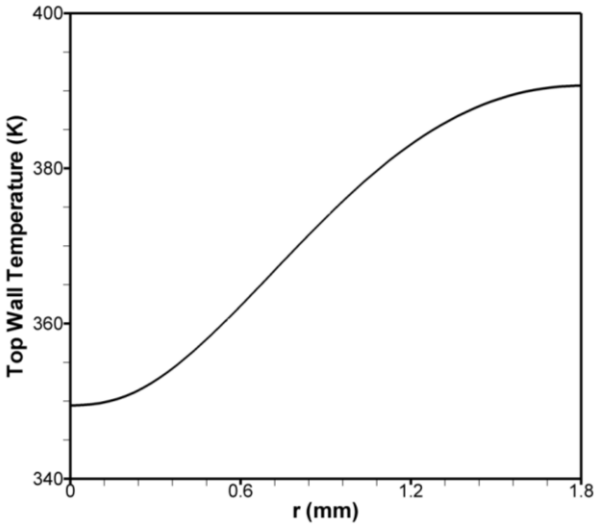

FIGURE 16. Temperature distribution of the top plate in the radial direction before the attachment of the drop, for a power input of 2 W.

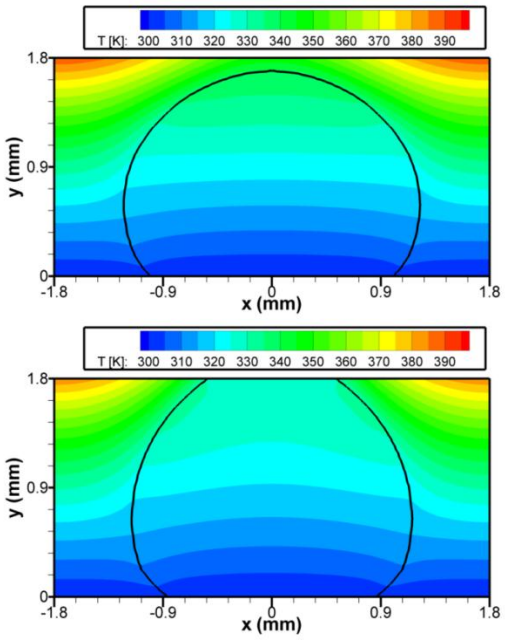

FIGURE 17. Temperature distribution of the system before (top) and after the attachment of the drop (bottom) when the voltage is removed, for a power input of 2 W. The free surface of the drop is shown with a black line inside the domain.

To increase the rate of heat transfer from the top plate in this case, the voltage should be removed similarly such that the drop will attach to the top plate. Figure 17 shows this action in which the temperature of the top plate experienced a 21 K decrease on the axis of symmetry. Also, the temperature at the periphery of the top plate decreased from 391 K to 385 K which shows that the effectiveness of the drop is higher in the regions where it is in contact with the top plate.

The comparison between the temperature distributions for the attached and detached conditions is demonstrated in Fig. 18. Similarly, the temperature of the central region of the top plate experienced a 21 K decrease, while this value for the peripheral region is only 6 K. It can be seen that the temperature of the part of the top plate in contact with the drop, is nearly constant against the radius of the top plate.

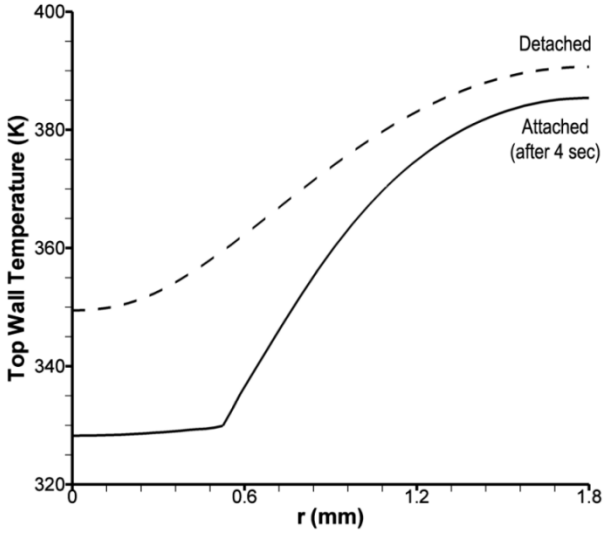

FIGURE 18. Comparison between the temperature distribution of the top plate in the radial direction before and after the voltage removal, for a power input of 2 W.

Based on the results presented above, it can be concluded that under similar conditions, the ability of the drop to reduce the temperature increases by adding more heat power to the top plate. As a result, the 6 µL drop is capable of cooling a hot spot with a 10mm^2 surface area and power input of 1 W by 11 K, whereas this value for a 2 W hot-spot can increase to 21 K.

CONCLUSION

In this paper, the possibility of designing an EWOD-based system was investigated by employing liquid metal drops in cooling of hot-spots in electronic devices. An experimental setup was designed to obtain the values of contact angle, apex and contact radius of a mercury drop with various sizes. These values were collected using a simple image-processing technique to study the behavior of the drop under a 240V electrical potential. The experimental results demonstrated that in comparison with a 6 µL drop, the obtained values for the contact angle and apex are less repeatable for a 2.8 µL drop. This finding suggested that the behavior of smaller drops under an applied voltage are influenced by the contact angle hysteresis and pinning phenomena and, therefore, smaller drops are not advised for a hot-spot cooling purpose. In addition, a numerical method was developed to simulate the electrowetting phenomenon in combination with the heat transfer formulations to study the effects of a drop in cooling hot-spots with various heat power inputs. Using this method, the profile of a 6 µL drop was simulated with and without an applied voltage of 240V and compared well with the experimental results. In addition, the results of the hot-spot simulation showed that a 6 µL drop is capable of cooling a hot-spot with a heat flux as high as 2 W out of a surface area of 10 mm^2 from 350 K to 328 K.

REFERENCES

[1] 2003 International Technology Roadmap for Semiconductors (ITRS), (2003). *Executive Summary*, page 57.

[2] Campbell Jr., J. S., Black, W. Z., Glezer, A., and Hartley, J. G., (1998), "Thermal Management of a Laptop Computer with Synthetic Air Microjet," *International Conference on Thermal, Mechanics, and Thermomechanical Phenomena in Electronic Systems (ITHERM)*, pp. 43–50.

[3] Go, J. S., Kim, S. J., Lim, G., Yun, H., Lee, J., Song, I., and Pak, Y.E., (2001), "Heat Transfer Enhancement Using Flow-Induced Vibration of Microfin Array," *Sensors and Actuators A*, **90**, pp. 232–239.

[4] Lippmann, G., (1875). "Relations Entre Les Phénomènes Électriques Et Capillaries," *Ann. Chim. Phys*. **5**, pp. 494-549.

[5] Pollack, M.G., Fair, R.B., Shenderov, A.D., (2000). "Electrowetting based actuation of liquid drops for microfluidicapplications," *Appl. Phy. Lett*. **77**, pp. 1725-1726.

[6] Berry, S., Kedzierski, J., and Abedian, B. (2006)., "Low Voltage Electrowetting Using Thin Fluoropolymer Films," *Journal of Colloid and Interface Science*, **303**, pp. 517-524.

[7] Song, J. H., Evans, R., Lin, Y. Y., Hsu, B. N., and Fair, R. B., (2008). "A Scaling Model for Electrowetting-On-Dielectric Microfluidic Actuators," *Microfluid Nanofluid*, **7(1)**, pp. 75-89.

[8] Keshavarz-Motamed, Z., Kadem, L., and Dolatabadi, A., (2009). "Effects of Dynamic Contact Angle On Numerical

Modeling of Electrowetting in Parallel Plate Microchannels," *Microfluid Nanofluid*, **8(1)**, pp. 47-56.

[9] Jang, L. S., Hsu, C. Y., and Chen, C. H., (2009). "Effect of Electrode Geometry on Performance of EWOD Device Driven by Battery-Based System," *Biomed Microdevices*, **11(5)**, pp. 1029-1036.

[10] Rajabi, N., and Dolatabadi, A., (2010). "A Novel Electrode Shape for Electrowetting-Based Microfluidics," *Colloids and Surfaces*, **365**, pp. 230-236.

[11] Alavi, S., Passandideh-Fard, M., and Tafteh, M. H., (2011). "Electrowetting Actuation For a Sessile Liquid Drop: Experiments and Simulations," *in Proceedings of the ASME 9th International Conference on Nanochannels, Microchannels, and Minichannels (ICNMM2011)*, 19-22 June, 2011, Edmonton, Canada.

[12] Quilliet, C., and Berge, B., (2001). "Electrowetting: A Recent Outbreak," *Current Opinion in Colloid & Interface Science*, **6**, pp. 34-39.

[13] Erickson, D., and Li, D., (2004). "Integrated Microfluidic Devices," *Analytica Chimica Acta*, **507**, pp. 11-26.

[14] Pamula, V.K., Chakrabarty, K., (2003). "Cooling of Integrated Circuits using Drop-Based Microfluidics," *Proc. ACM Great Lakes Symposium on VLSI*, pp. 84-87.

[15] Paik, P.,Pamula, V. K.,Chakrabarty, K., (2005). "Drop-Based Hot Spot Cooling using Topless Digital Microfluidic on a Printed Circuit Board," *TIMA EDITIONS / THERMINIC*, pp.1-4.

[16] Mohseni, K., (2005). "Effective Cooling of Integrated Circuits using Liquid Alloy Electrowetting," in Proceedings of the 21st SEMITHERM Symposium, San Jose, USA, pp. 20–25.

[17] Paik, P. Y., (2006). "Adaptive Hot-Spot Cooling of Integrated Circuits Using Digital Microfluidics," Ph.D. Thesis, Department of Electrical and Computer Engineering, Duke University, Durham, NC.

[18] Cheng, J. T., and Chen, C. L., (2010). "Active Thermal Management of On-Chip Hot-Spots Using EWOD-Driven Drop Microfluidics," *Exp. Fluids*, **49**, *Springer*, Research Article.

[19] Oprins, H., Danneels, J., Van Ham, B., Vandevelde, B., and Baelmans, M., (2008). "Convection Heat Transfer in Electrostatic Actuated Liquid Drops for Electronics Cooling," *Microelectronics Journal*, **39**, pp. 966–974.

[20] Paik, P. Y., Chakrabarty, K., and Pamula, V. K., (2007). "*Adaptive Cooling of Integrated Circuits Using Digital Microfluidics*," Artech House Inc., Norwood, USA.

[21] Mirzaii, I., and Passandideh-Fard, M., (2011). "Modeling free surface flows in presence of an arbitrary moving object," *Int. J. Multiphase Flow*, (in press).

[22] Kershaw, D.S., (1978). "The Incomplete Cholesky-Conjugate Gradient Method for the Iterative Solution of Systems of Linear Equations," *Journal of Computational Physics*, **26(1)**, pp. 43-65.

[23] Youngs, D.L., (1984). "An Interface Tracking Method for a 3D Eulerian Hydrodynamics Code," Technical report 44/92/35, AWRE.

[24] Brackbill, J.U., Kothe, D.B., and Zemach, C., (1992). "A Continuum Method for Modeling Surface Tension," *Journal of Computational Physics*, **100(2)**, pp. 335-354.

[25] Aleinov, I., and Puckett, E.G., (1995). "Computing Surface Tension With High-Order Kernels," *Sixth International Symposium on Computational Fluid dynamics*, Lake Tahoe, NV, pp. 13-18.

[26] Carslaw, H.S. and Jaeger, J. C., (1975). "*Conduction of Heat in Solids*," Oxford University Press, London.

[27] Shamsunder, N. and Sparrow, E.M., (1975). "Analysis of Multidimensional Conduction Phase Change via the Enthalpy Model," *J. Heat Transfer*, **97(3)**, pp. 333-340.

[28] Johnson, R. E., and Dettre, R. H. (1964)., "*Contact Angle Hysteresis I: Study of an Idealized Rough Surface*," ACS Publications, pp. 112-135

[29] Huh, C., and Mason, S. G., (1977). "Effect of Surface Roughness on Wetting (Theoretical)," *Journal of Colloid and Interface Science*, **60(1)**, pp. 11-38.

[30] Zisman, W. A., (1964). "Relation of the Equilibrium Contact Angle to Liquid and Solid Constitution," *ACS Adv. Chem.*, **43(1)**, pp. 1-51.